Smart Structures and Systems, *Vol. 19, No. 2 (2017) 137-149*
DOI: https://doi.org/10.12989/sss.2017.19.2.137

Elimination of environmental temperature effect from the variation of stay cable force based on simple temperature measurements

Chien-Chou Chen[*1], Wen-Hwa Wu[1a], Chun-Yan Liu[2b] and Gwolong Lai[1c]

[1]Department of Construction Engineering, National Yunlin University of Science and Technology, 123 University Road, Touliu, Yunlin 640, Taiwan
[2]Graduate School of Engineering Science and Technology, National Yunlin University of Science and Technology, 123 University Road, Touliu, Yunlin 640, Taiwan

(Received June 24, 2016, Revised October 20, 2016, Accepted October 27, 2016)

Abstract. Under the interference of the temperature effect, the alternation of cable force due to damages of a cable-stayed bridge could be difficult to distinguish. Considering the convenience and applicability in engineering practice, simple air or cable temperature measurements are adopted in the current study for the exclusion of temperature effect from the variation of cable force. Using the data collected from Ai-Lan Bridge located in central Taiwan, this work applies the ensemble empirical mode decomposition to process the time histories of cable force, air temperature, and cable temperature. It is evidently observed that the cable force and both types of temperature can all be categorized as the daily variation, long-term variation, and high-frequency noise in the order of decreasing weight. Moreover, the correlation analysis conducted for the decomposed variations of all these three quantities undoubtedly indicates that the daily and long-term variations with different time shifts have to be distinguished for accurately evaluating the temperature effect on the variation of cable force. Finally, consistent results in reducing the range of cable force variation after the elimination of temperature effect confirm the validity and stability of the developed method.

Keywords: stay cable force; air temperature; cable temperature; ensemble empirical mode decomposition; daily variation; long-term variation

1. Introduction

It is an extremely important issue to maintain the safety and serviceability of critical civil structures such as long-span bridges. Although visual inspection or experimental methods were often adopted for structural condition assessment, their applications in bridges are generally restricted to the accessible and pre-known local portions of structure with high damage potential. Recently, more studies have aimed to develop global structural safety assessment and damage detection methods. Several of them revealed that structural health monitoring (SHM) is one of the feasible solutions to effectively evaluate the structural condition (Cunha, Caetano *et al*. 2013, Trker and Bayraktar 2014) or detect different degrees of damages (Whelan and Janoyan 2010, Cunha, Caetano *et al*. 2013, Dohler, Hille *et al*. 2014) for bridges. Even so, the accuracy of SHM techniques in practical applications for bridge damage diagnosis remains to be extensively verified and further improved.

For cable-stayed bridges, it is apparent that the most crucial structural component is the stay cable system because it suspends most of girder weight and is the primary path for transmitting the live loadings on girder. Consequently, the abnormal change in structural condition for a cable-stayed bridge would naturally lead to the force redistribution of its cable system and the monitoring of cable force can be regarded as a royal road to diagnose the possible damages. The ambient vibration method is most commonly employed for monitoring the tension of stay cable because of its convenient operation and wide applicability. This method is typically applied with first identifying the cable frequencies from vibration measurements and then using a pre-determined formula to estimate the cable force. A big challenge to the success of such a cable force monitoring approach is that environmental effects may also play a major role in the variation of cable force along with damages. Under the interference of these environmental effects, the alteration of cable force due to damages could be difficult to distinguish.

Quite a few studies for cable-stayed bridges clearly indicated that temperature is usually the key environmental factor to induce the variation in the modal frequencies of bridge (Ni, Hua *et al*. 2005, Min, Sun *et al*. 2009), the expansion joint displacement (Ni, Hua *et al*. 2007) or the cable frequencies (Degrauwe, De Roeck *et al*. 2009, Chen, Wu *et al*. 2010). Therefore, the applicability of the above-

*Corresponding author, Associate Professor
E-mail: ccchen@yuntech.edu.tw
[a] Professor
E-mail: wuwh@yuntech.edu.tw
[b] Ph.D. Student
E-mail: g9910817@yuntech.edu.tw
[c] Associate Professor
E-mail: laig@yuntech.edu.tw

ISSN: 1738-1584 (Print), 1738-1991 (Online)

mentioned SHM approach to cable-stayed bridges deeply depends on accurate quantification of this influence. Based on the observation data of a PC cable-stayed bridge, Li (2009) extensively examined various aspects of possible temperature influences including the temperature change of the whole bridge, the temperature difference between cable and main girder, the temperature gradient in the transverse section of main girder, and the temperature gradient in the transverse section of pylon. With one-year monitoring data of a cable-stayed bridge, Min, Sun *et al*. (2011) analyzed the distribution characteristics of environmental temperature to find that it was uniformly distributed along the longitudinal direction of bridge and there existed a significant temperature gradient in the cross section of box girder. By inspecting the thermal time lags and gradients of the steel box girder, concrete tower, and stayed cables, Cao, Yim *et al*. (2011) indicated that the concrete temperature lagged significantly behind that of the ambient air and the cable temperature usually proceeded between them. Ding, Wang *et al*. (2013) recently probed the statistical characteristics of temperature and the thermal differences in the flat steel box girder section of a cable-stayed bridge. Further efforts were also made to simulate the environmental temperature effect by (1) approximately considering an equivalent alteration in the material and structural behaviors (Ni, Zhou *et al*. 2008); (2) developing a correlation model between the modal frequencies and environmental temperatures (Ni, Zhou *et al*. 2009); or (3) constructing appropriate input with mean temperatures, effective temperatures, and principal components of temperatures to neural networks (Zhou, Ni *et al*. 2010). Using the correlation model formulated with the back-propagation neural network technique, Zhou, Ni *et al*. (2012) even attempted to normalize the modal frequencies measured under different temperature conditions to an identical reference status of temperature for eliminating the temperature effect. Relatively few of these works (Degrauwe, De Roeck *et al*. 2009, Li 2009, Cao, Yim *et al*. 2011), however, were focused on investigating the cable force variation caused by the change of temperature. Moreover, the live loading from traffic is also considered as the other main environmental factor to alter the structural condition of a cable-stayed bridge. Certain researches have been conducted to evaluate the effect of traffic load on the variation of cable force, but mostly focusing on assessing the fatigue strength of stay cable (Li, Ou *et al*. 2009, Li, Ou *et al*. 2012, Li, Li *et al*. 2014, Li and Ou 2016). Compared to the gradual and fairly regular trend coming from the environmental temperature effect, the traffic load normally creates a prompt and irregular variation in cable force. Even though it was ever reported (Li and Ou 2016) that the effect of traffic load on the stay cable force can be more dominant than that of temperature for a cable-stayed bridge in China, particular notice should be made on the fact that this analysis was based on the data collected from a bridge usually subjected to overloaded trucks as heavy as 190 tons.

Theoretically, the temperature effect can be accurately investigated if the comprehensive temperature field of the structural system is available to consider intricate phenomena such as the thermal gradient. This sort of analysis, however, is generally not feasible for the health monitoring of a real structure because it would require a tremendous amount of temperature sensors to be installed on the structure. For practically assessing the variation of cable force induced by the environmental temperature variation, a recent study by the authors conducted a long-term monitoring on the cable forces and temperatures in various structural components of Ai-Lan Bridge, a low-pylon cable-stayed bridge located in central Taiwan (Chen, Wu *et al*. 2012, Chen, Wu *et al*. 2016). Considering the structural characteristics associated with this type of bridges like the high flexural rigidity of strong girders and the relatively low thermal conductivity of concrete members, this work adopted an effective temperature index to globally incorporate all the contributions from stay cable, bridge girder, and pylon according to appropriate geometrical setup. It was discovered that this effective temperature is strongly correlated with the cable force. More importantly, the residual cable force variation after eliminating the environmental temperature effect was limited to a narrow range such that sensitive criteria can be constructed for successful damage detection (Chen, Wu *et al*. 2016). It is also noteworthy that the traffic load effect was not found to be a crucial factor in the above study due to two principal reasons. First, the determination of cable force in that research was based on the ambient vibration method by processing 300 sec of cable vibration signal with the discrete Fourier transform (DFT) technique. Under such circumstances, the drastic effect coming from the instantaneous traffic load would be smoothed and averaged, as also indicated in the literature (Li and Ou 2016). In addition, it has been validated that the range of cable force variation for Ai-Lan Bridge is relatively small under standard live loading. The load test with four trucks of 30 tons conducted before the operation of this bridge was found to induce approximately 0.5% of cable force variation.

Focusing on the convenience and economy in engineering practice of structural health monitoring, the current work further explores the possibility of eliminating the environmental temperature effect merely with simple cable or air temperature measurements. The empirical mode decomposition (EMD) is applied to process the time histories of cable force, air temperature and cable temperature for a more detailed investigation of their correspondence. EMD was first proposed by Huang et al. in 1998 (Huang *et al*. 1998) for decomposing a signal totally in accordance with its own characteristics and scales. The core concept of EMD is to decompose the original signal into several intrinsic mode functions (IMF) by the sifting process. More specifically, it does not need to perform the decomposition with pre-determined bases such as the sinusoidal functions in Fourier analysis and the mother wavelets in the wavelet analysis. Due to this adaptive feature, EMD can be expediently applied to deal with non-stationary (Hu, Yang *et al*. 2008, He, Hua *et al*. 2011) and nonlinear (Chang and Poon 2010, Pai 2013) signals. While simply with a history of less than two decades, EMD has rapidly developed into a popular signal processing tool utilized in various research fields. Taking civil engineering for instance, widespread applications in structural system identification (Chang and Poon 2010, Yu and Ren 2005, Yang and Chang 2009, Chen 2009), damage detection (Chen 2009, Dong, Li *et al*. 2010, Rezaei and Taheri 2011, Bagherzadeh and Sabzehparvar 2015), and health monitoring of bridges (He, Hua *et al*. 2011, Yu and Ren 2005, Yang and Chang 2009, Chen 2009, Lee, Wu *et al*. 2003, Lin 2011, Zhang, Du *et al*. 2012) have been increasingly reported. Performing EMD and its noise-assisted version, ensemble empirical mode decomposition (EEMD), the corresponding IMF's for the time histories of cable force and those for the cable or air temperature are closely examined in this study. Such elaborate procedures are intended to more effectively categorize different components of the cable force, cable temperature and air temperature for further denoising and more specific correlation analyses. With these decomposed IMF's, the correlation coefficients between the cable force and the cable or air temperature are then computed for various possible combinations to find the best correlated components of the two investigated quantities. Furthermore, the results for three stay cables of Ai-Lan Bridge with different lengths in each of the four seasons are presented and compared to verify the general applicability of the proposed methodology.

2. Measurements of cable force and temperatures for Ai-Lan Bridge

Due to the consideration of landforms, several low-pylon cable-stayed bridges have been recently constructed in Taiwan. Ai-Lan Bridge with a main span of 140m, as shown in Fig. 1(a), is one of these examples. Its cable system is arranged in a harp shape along the centerline of girder with nine pairs of stay cables on each side of every pylon, as illustrated in Fig. 1(b). The pylon is a single solid concrete post, rigidly connecting with the prestressed concrete box girder. Each stay cable is composed of parallel strands inside HDPE tube with grouting and both of its ends are anchored to the tower or girder by the OVM HYDIN type of anchorage. The bridge commenced its construction in 2004 and was opened for traffic in 2008. A monitoring system was established during its construction stage. The function of the monitoring system is to measure the stress and/or strain conditions of critical bridge components as well as the temperature variations of surrounding air, girder and pylon.

In addition to the existing monitoring system, a simple device composed of a fiber Bragg grating (FBG) sensor attached on a fishing line (Chen, Wu *et al*. 2008) was developed by this research group to adequately measure the ambient vibration signals of the cable system and is shown in Fig. 2(a). These FBG sensors were installed on Cables E1 to E18, all the 9 pairs of cables on G2 side of Pylon P1. From those signals, the natural frequencies of each cable can be identified and then employed to determine the corresponding cable forces with the ambient vibration method. As for the temperature measurements, a number of thermocouples were installed at six cross sections of girder and two cross sections of pylon in the original monitoring system to measure the structural temperature. Besides, several thermometers were also deployed outside and inside three selected cross sections of girder to record the air temperature. No temperature sensors, however, were aimed at taking the cable temperature in the original monitoring system. To fit this cavity, a cable specimen of 1 m long was also made by this research group for imitating the real cable by assembling the same number of tendons inside an HDPE tube (Chen, Wu *et al*. 2012) and is exhibited in Fig. 2(b). FBG temperature sensors were attached on the surface of four inside tendons to intimately take the temperature of the cable specimen placed on the bridge deck.

(a) Photograph

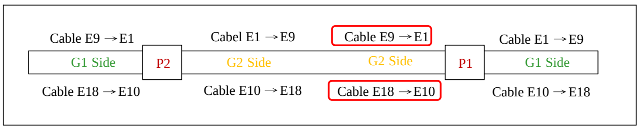

(b) Illustration of cable arrangement

Fig. 1 Cable system of Ai-Lan Bridge

(a) For cable vibration

(b) For cable temperature

Fig. 2 Measurement devices with FBG sensors

With this measurement system, the vibration signal from the FBG sensor installed on each cable was automatically collected for 300 sec every 15 minutes at a sampling rate of 250 Hz. The temperature variation can cause observable wavelength shifts in the FBG sensors to interfere with the measurement of cable vibration. This effect, however, is very limited in the short duration of 5 minutes and consequently neglected in the current study. The measured displacement time history of cable vibration is first transformed into the frequency domain by the DFT technique. The cable frequencies can then be clearly identified.

3. Variations of different temperatures and stay cable force

Fig. 3 depicts a typical example illustrating the daily temperature variations of air and various structural components. It is apparently observed from this figure that the daily temperature variations at different locations share a similar fluctuation curve mainly composing of a steeper increasing trend during the daytime and the other slower decreasing trend during the nighttime. Nonetheless, closer examination discloses two major distinctions in variation magnitudes and time lags among these different temperature measurements. As far as the daily variation magnitude is concerned, the air temperature exhibits a larger value than that for the cable and those for the girder and pylon are much smaller than the former two. The main reason for a lower temperature variation of cable than that of air is because the strands are encased in a HDPE tube with grouting. In fact, this is also the reason why the cable temperature obviously evolves in a smoother way than the air temperature. On the other hand, the temperatures of various structural components all demonstrate time lags in the daytime rising curve with respect to the corresponding air temperature. More specifically, the significance of this time lag in temperature follows the order of girder, cable, and pylon. It should be noted that the above trends are consistently held all year round from inspecting the data covering one year and similar to those reported by Cao, Yim *et al*. (2011). The exceptions only occur in the days under cold fronts to considerably reduce the variation magnitude and spoil the daytime increasing trend. As mentioned in Section 1, the exact heat transfer mechanisms among different structural components would not be explored in this study due to its great complexity. Instead, the investigation will be focused on the effects of various temperature variations.

Based on the string theory where the effects of cable sag and flexural rigidity are considered negligible, the internal force F_0 of a stay cable at a reference time t_0 can be expressed in terms of its modal frequency as

$$F_0 = 4\overline{m}L^2\left(\frac{f_{n0}}{n}\right)^2 \text{ or } \varepsilon_0 = \frac{F_0}{EA} = \frac{4\overline{m}L^2}{EA}\left(\frac{f_{n0}}{n}\right)^2 \qquad (1)$$

where L, $\overline{m}$, E and A represent the length, mass per unit length, Young's modulus and cross-sectional area of cable, respectively; f_{n0} signifies the natural frequency of the n-th mode in Hz and ε_0 symbolizes the axial strain, both at the reference time. It can also be noted from Eq. (1) that the cable force is proportional the square of the cable frequency. Considering the corresponding quantities F_i, f_{ni} and ε_i at any other time instant t_i, subtraction of the two sets of quantities at different time instants directly yields

$$\frac{\Delta F}{F_0} = \frac{F_i - F_0}{F_0} = \frac{f_{ni}^2 - f_{n0}^2}{f_{n0}^2} = \frac{\Delta f_n^2}{f_{n0}^2} = \frac{\varepsilon_i - \varepsilon_0}{\varepsilon_0} = \frac{\Delta\varepsilon}{\varepsilon_0} \qquad (2)$$

It is well known that the change of structural temperature can directly induce the variations in internal stress and strain of a structural system. In a recent work for evaluating the variation of cable force caused by the environmental temperature effect (Chen, Wu *et al*. 2012, Chen, Wu *et al*. 2016), the authors proposed an effective temperature index to combine all the contributions from stay cable, bridge girder and pylon. It is attempted in the current study to further simplify such an approach by adopting a single temperature measurement. As suggested from Fig. 3, either the air temperature variation ΔT_a or that of cable ΔT_c is generally more significant than those of the other bridge components and will be separately taken to serve as a simple temperature index for eliminating the environmental temperature effect from the variation of cable force.

Considering the nearly equally-spaced distribution for different modal frequencies of a stay cable, any single cable frequency is eligible for indicating $\Delta F/F_0$. A statistical analysis was performed with the collected data from the first month to determine the most significant mode usually observed for each cable. The results of this analysis led to the uniform choice of the first modal frequency for each cable in the subsequent investigations (Chen, Wu *et al*. 2012). As an example to illustrate the relationship between the cable force variation and either of the two simple temperature indices, $\Delta f_n^2/f_{n0}^2$ (n = 1) to represent $\Delta F/F_0$ is plotted in Fig. 4 together with the variations of air temperature and cable temperature for a typical day. It should be noted that the ordinates for ΔT_a and ΔT_c are defined in an opposite direction to that for $\Delta F/F_0$. This is particularly designed such that the negative correlation between $\Delta F/F_0$ and ΔT_a or ΔT_c can be easily compared. From Fig. 4, it is evident that $\Delta F/F_0$ follows a consistent trend with either ΔT_a or ΔT_c.

Nevertheless, an emphasis needs to be made that such a tendency may be only valid for the investigated low-pylon cable-stayed bridge with a strong girder. Regarding the other cases of conventional cable-stayed bridges, the load redistribution caused by the increase of temperature might enlarge the force of certain cables.

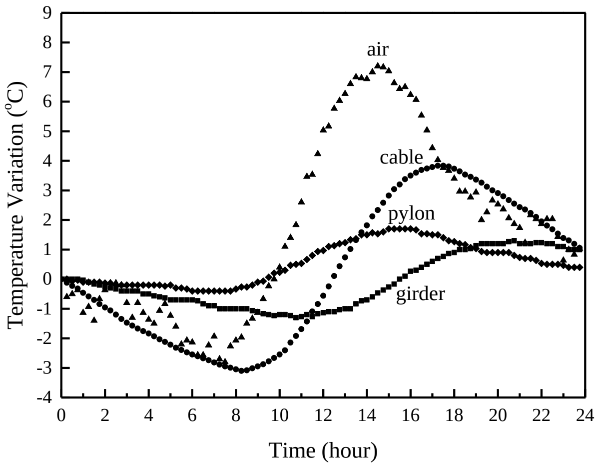

Fig. 3 Daily temperature variations of air and various structural components

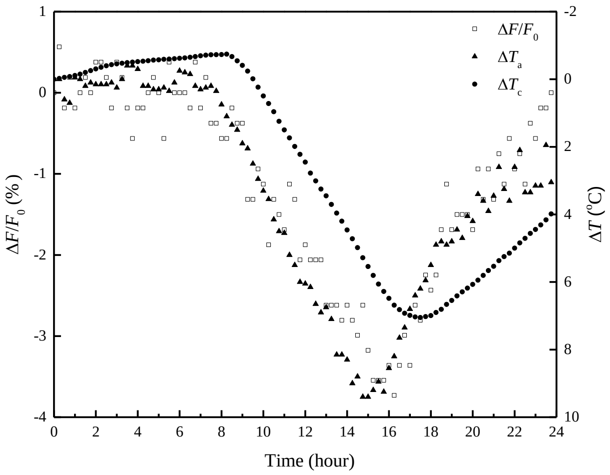

Fig. 4 Daily variations of cable force, air temperature and cable temperature

Another interesting observation from Fig. 4 is that there exists certain time shift between the variation of cable force and that of air temperature or cable temperature. The air temperature firstly reaches its daily maximum at around 3PM, followed by the minimum cable force occurring at about 4PM and then the peak cable temperature after 5PM. Other than demonstrating the strong correlation between $\Delta F/F_0$ and ΔT_a or ΔT_c, Fig. 4 further reveals that the traffic load effect may cause the high-frequency fluctuation in the cable force variation and is not comparable to the dominant temperature effect. In other words, the instantaneous effect of traffic load is significantly diluted by applying the ambient vibration method to determine the cable force. This consequence is certainly beneficial to the subsequent elimination of environmental temperature effect from the cable force variation and the residual variation after elimination would at least partially reflect the smoothed effect of traffic load.

4. Decomposition of different temperatures and stay cable force

Although the results in Fig. 4 indicate a strong negative correlation between the cable force and the air temperature or the cable temperature for a duration of one day, the long-term temperature effect on the cable force requires further exploration. Because of several technical problems ever encountered with the installed FBG system, there were totally 223 days of effective signals intermittently collected from September of 2010 to August of 2011. Fortunately, approximately one month of continuous data can still be extracted for each of the four seasons (30 days in the spring, 21 days in the summer, 22 days in the autumn, and 30 days in the winter). To more systematically investigate their correspondence, an effective decomposition method is needed to distinguish the daily and long-term effects. The empirical mode decomposition is first adopted in this study to process the time histories of cable force, air temperature and cable temperature.

4.1 Empirical mode decomposition

EMD is an adaptive method to decompose a signal into several intrinsic mode functions in balanced oscillations with respect to their zero means. The procedures of EMD usually start with constructing the upper and lower envelopes of the original signal by performing cubic spline interpolations to fit the local maxima and minima, respectively. The average of both envelopes can then be taken to determine a temporary baseline, which is subtracted from the original signal to complete the first round of sifting process. By repeatedly conducting such a sifting process until the number of zero crossings is very close to that of extrema, an IMF can eventually be obtained. Subsequently, subtraction of the extracted IMF from the original signal is carried out to yield the remained signal ready for decomposing the next IMF by similar sifting procedures. This process is reiterated until a monotonic signal, usually referred as the residue, is remained. Overall, the empirical mode decomposition of a signal can be mathematically expressed as

$$s(t) = \sum_{k=1}^{m} c_k(t) + r(t) \tag{3}$$

where $s(t)$ is the original signal, $c_k(t)$ is the k-th IMF, $r(t)$ is the residue, and m signifies the total number of obtained IMF's. It should be emphasized that the IMF’s coming from the EMD process earlier usually have the content in a higher frequency range. Furthermore, the narrow-banded frequency content may not be guaranteed for each IMF due to the adaptive nature of this method.

Taking the one-month data of Cable E13 measured in the winter and shown in Fig. 5 for example, the IMF’s obtained from the EMD process for the variations of air temperature, cable temperature and cable force are shown in Figs. 6 to 8. It is clear that the first three IMF’s of air temperature variation and the first IMF of cable temperature variation are composed of extremely high-frequency components, which are not possible to be present in temperature variation and should be considered as measurement noises. Therefore, these IMF’s are excluded from the temperature history in the subsequent correlation analysis for identifying all the IMF’s of cable force closely related to the temperature variation. All the possible combinations of cable-force IMF’s are checked to examine their correlation with the denoised temperature. It is found that the highest correlation coefficient of 0.79 with the air temperature and 0.58 with the cable temperature can be obtained by combining IMF 5 of cable force up to the residue. This result discloses that the cable force components from IMF 5 to the residue are most related to the effect of temperature variation and the first four IMF’s should come from the sources such as measurement noises or traffic loads.

As illustrated in Fig. 4, there exists a clear time shift between the variation of cable force and that of cable temperature. An optimal time shift of 3.0 hr (12 time increments of 15 minutes) can then be determined to improve the correlation coefficient between the denoised histories of cable temperature and cable force from 0.58 to 0.75. Even so, enhancement can still be anticipated to further increase the corresponding correlation coefficient since Figs. 7 and 8 also show that the other minor IMF's of cable force do not correspond well with those of cable temperature, not to mention the feasibility of obtaining appropriate time shifts. In fact, it is not difficult to accept that the temperature variation in a whole year should be at least distinguished into the daily variation and the long-term variation. Accordingly, the correlation would be undoubtedly raised if it is able to distinctively classify the temperature effect on the cable force variation into daily and long-term bases. Figs. 6 to 8, however, exhibit another crucial problem that a wide range of frequency components may be mixed together in an IMF resulted from the EMD process. To tackle this difficulty and then provide a better basis for discriminating the temperature effect on the cable force variation, the technique of ensemble empirical mode decomposition (EEMD) recently developed (Wu and Huang 2009) is further employed in this study.

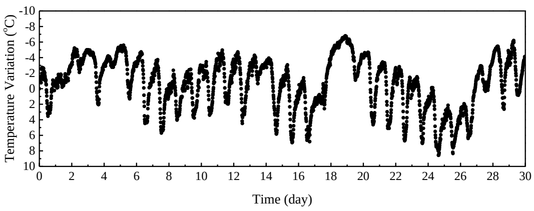

(a) Air temperature

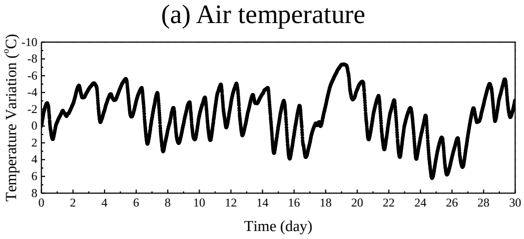

(b) Cable temperature

Continued-

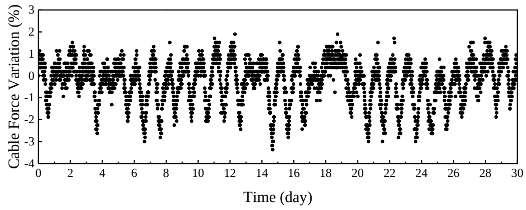

(c) Cable force

Fig. 5 One-month data of Cable E13 measured in the winter

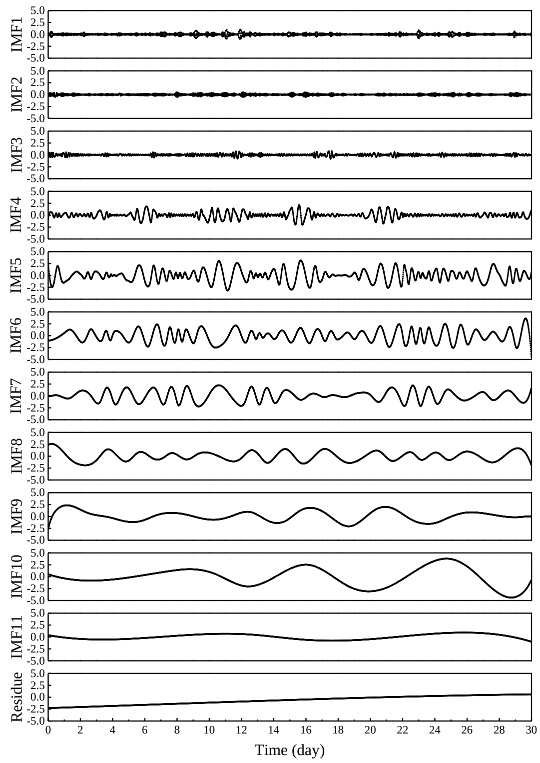

Fig. 6 IMF’s of the air temperature variation in the winter from EMD

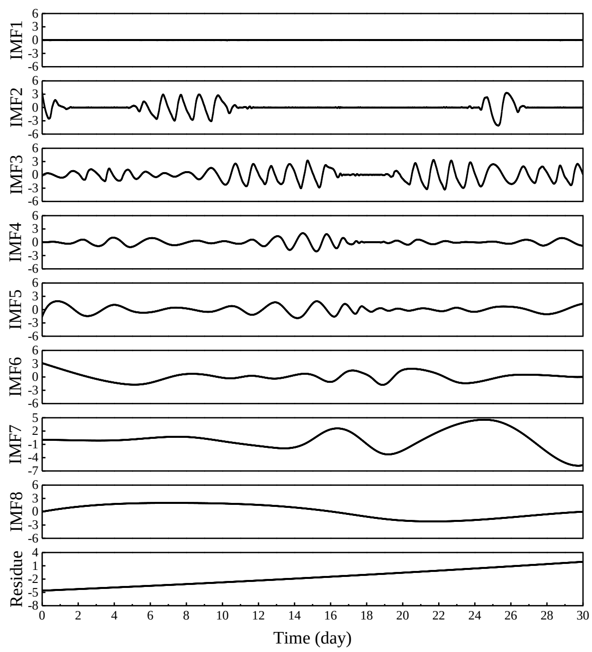

Fig. 7 IMF’s of the cable temperature variation in the winter from EMD

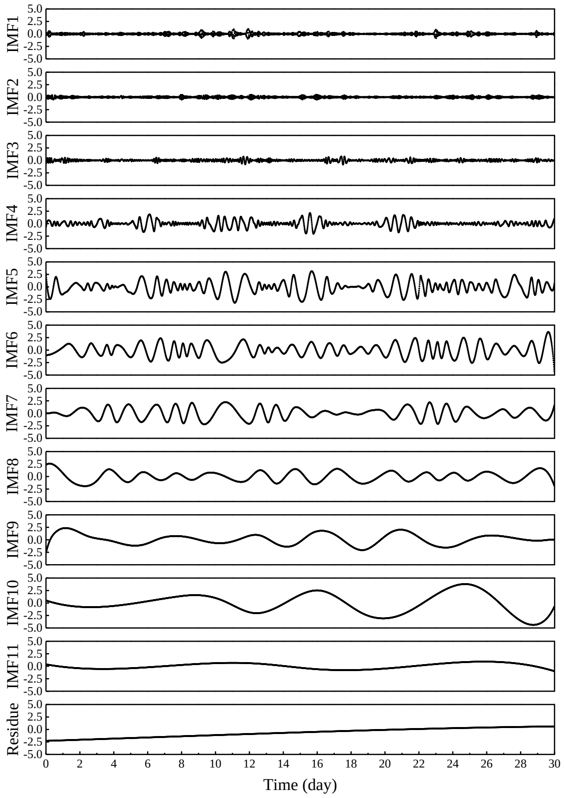

Fig. 8 IMF’s of the cable force variation for Cable E13 in the winter from EMD

4.2 Ensemble empirical mode decomposition

Modified from EMD, EEMD is a noise-assisted data analysis method to ensure the narrow-banded frequency content for each IMF. The procedure of EEMD starts with adding a white noise with a zero mean and a standard deviation of certain level to the targeted signal. The noise-added signal is then decomposed into several IMF’s with the conventional EMD process. Such an operation is repeatedly conducted with different random white noises to produce numerous sets of IMF’s. Finally, the average of all the corresponded IMF’s in different sets is taken to determine the final version of each specific IMF. It is noteworthy that the purpose of adding a white noise to the original signal is to help create a uniform distribution in the frequency domain for generating well separated and narrow-banded IMF’s. Although the individual EMD processes may yield the IMF’s highly polluted by the added noises, all the artificial noises would be eventually cancelled out in the final averaging operation as long as the ensemble number is sufficiently large. It is no doubt that the EEMD process is much more time-consuming than the conventional EMD process and its computation cost increases with the ensemble number. To minimize such a disadvantage, the adoption of paired white noises with opposite values at each instant is introduced in the current study. With this setup, the perfect cancellation of noises can still be guaranteed all along the time history even if a significantly reduced ensemble number is taken.

For the same one-month data in the winter, the goal of creating well separated and narrow-banded IMF’s can be easily achieved simply with 10 pairs of random white noises. Another important parameter to be determined in the EEMD process is the level of standard deviation for the added white noises. This noise level needs to be comparable with the amplitude of the original signal such that the addition of noise can induce the expected effect. For the previously discussed time histories of air temperature, cable temperature and cable force, it is found that the noise level selected at 150% of the standard deviation of the original signal would consistently produce 11 stable IMF’s together with the residue from the EEMD process. The IMF’s resulted from the EEMD process for the variations of air temperature, cable temperature and cable force are depicted in Figs. 9 to 11, respectively. It should be noted that the first four IMF’s for these three quantities are all high-frequency noises and will be filtered out in the subsequent analysis. Comparison of Figs. 9 to 11 with Figs. 6 to 8 obviously verifies the success of applying EEMD. Furthermore, it is clear from the IMF's in Figs. 9 to 11 that IMF 5 to IMF 8 of the air temperature, the cable temperature and the cable force are all primarily contributed by the frequency components at 1 cycle/day and 2 cycle/day. Accordingly, the combination of IMF 5 up to IMF 8 for the air temperature or the cable temperature is believed to represent the daily temperature variation. On the other hand, the remained IMF 9 up to the residue in Fig. 9 or Fig. 10 naturally indicate the long-term temperature variation.

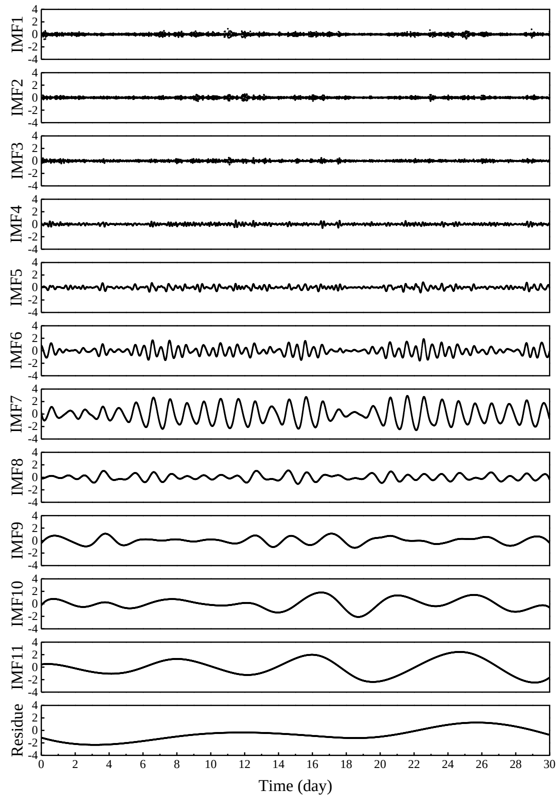

Fig. 9 IMF’s of the air temperature variation in the winter from EEMD

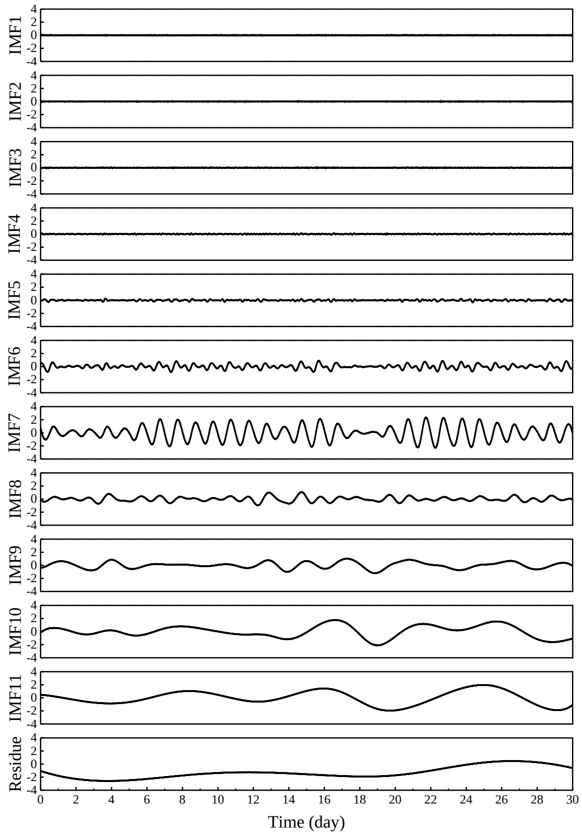

Fig. 10 IMF’s of the cable temperature variation in the winter from EEMD

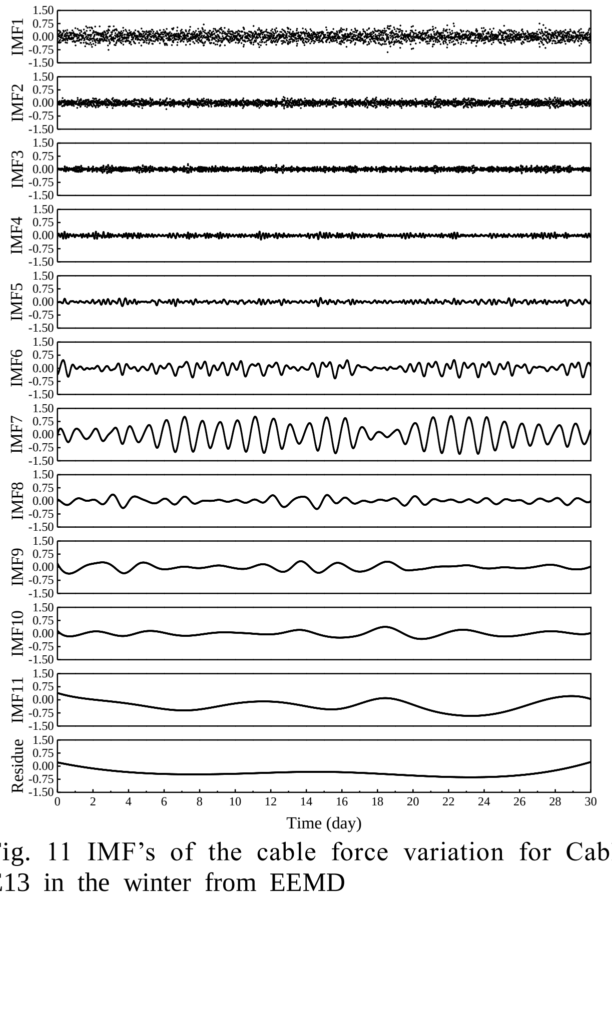

Fig. 11 IMF’s of the cable force variation for Cable E13 in the winter from EEMD

5. Correlation analysis

After classifying the air temperature into three parts including the daily variation, the long-term variation, and the high-frequency noise, the correlation analysis is again conducted between each of the first two major parts and any possible combination for the IMF's of the cable force with the consideration of optimal time shift. The same analysis is also performed for investigating the correlation between the cable temperature and the cable force. With no surprise, the combination of IMF 5 to IMF 8 for the cable force, with similar frequency contents to those for the air temperature, holds the maximum correlation coefficient of 0.96 under a time shift of 0.25 hr. Alternatively, the maximum correlation coefficient of 0.97 is attained under a time shift of 2.75 hr if the cable temperature is considered. These daily variations for the air temperature, the cable temperature and the cable force are displayed in Figs. 12(a) to 12(c), respectively. Such a high value of correlation coefficient evidently indicates the almost perfect correlation between the daily variations of cable force and either of the two considered temperature quantities. In addition, it needs to be mentioned that the positive value of time shift signifies the moving of cable force toward the later time instant, while the negative value denotes the opposite. As for the long-term variation, the combination of IMF 9 up to the residue for the cable force is also found to correlate best with those for the air temperature at a coefficient of 0.82 under a time shift of 10.5 hr. Moreover, the maximum correlation coefficient of 0.83 is obtained under a time shift of 16.5 hr if the cable temperature is adopted. Those long-term variations for the air temperature, the cable temperature and the cable force are illustrated in Figs. 13 (a) to 13(c), respectively. Detailed results for varying different time shifts also reveal that the correlation coefficient is quite sensitive to the time shift in the case of daily variation with a range from 0.96 to 0.40 for the air temperature and 0.97 to 0.22 for the cable temperature in ±4 hour, but seems to be insensitive with the alternation of time shift in the case of long-term variation.

Aside from the one-month data of Cable E13 measured in the winter as previously discussed, the corresponding data for the other three seasons are also taken to perform EEMD decompositions and the subsequent correlation analysis. The same procedures are further applied to analyze the other two cables, Cable E10 (shorter than Cable E13) and Cable E17 (longer than Cable E13). Table 1 summarizes the values of correlation coefficient in different cases together with the associated optimal time shifts listed in the parenthesis. All the values of correlation coefficient for different cases of daily variation using the air temperature are no less than 0.91 with optimal time shifts ranging from 1.5 to 0.5 hr.

The corresponding values of correlation coefficient employing the cable temperature are all above 0.97 with optimal time shifts ranging from 1.25 to 3.0 hr. On the other hand, the values of correlation coefficient associated with various cases of long-term variation are in the interval from 0.34 to 0.89 for the air temperature and from 0.52 to 0.89 for the cable temperature. Additionally, a time shift spanning from 6.5 to 27.25 hr and the other from 10.75 to 23.5 hr are observed for the air temperature and the cable temperature, respectively. Since the correlation coefficient is not sensitive to the time shift for the long-term variation, such a wide range of optimal time shifts is not surprising.

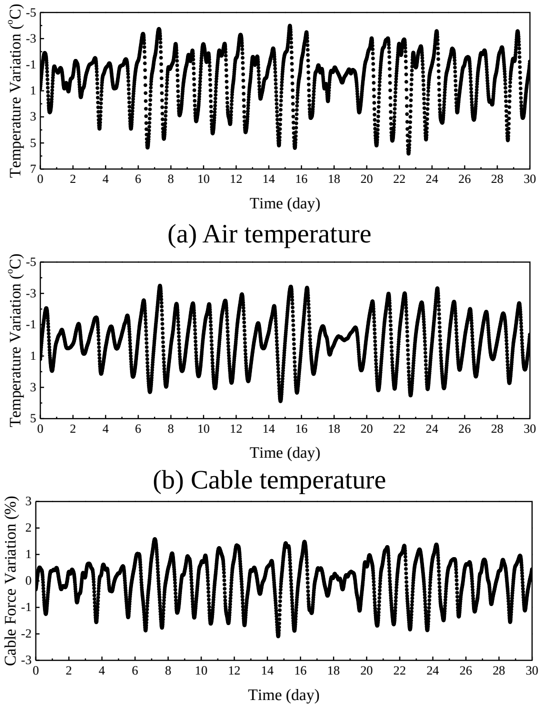

(a) Air temperature

(b) Cable temperature

(c) Cable force

Fig. 12 Daily variations for Cable E13 in the winter

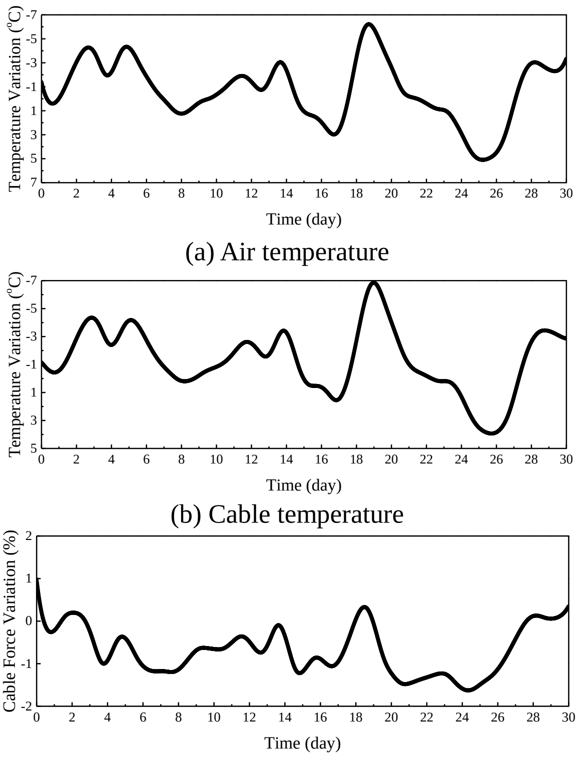

(a) Air temperature

(b) Cable temperature

(c) Cable force

Fig. 13 Long-term variations for Cable E13 in the winter

Table 1 Correlation coefficients and optimal time shifts for different seasons of three cables

Cable No.	Season	Correlation coefficient (optimal time shift in a unit of hr)			
		Daily variation		Long-term variation	
		Air temperature	Cable temperature	Air temperature	Cable temperature
E10	Spring	–0.94 (–0.75)	–0.98 (1.25)	–0.77 (19.75)	–0.85 (15.5)
	Summer	–0.91 (–0.5)	–0.97 (1.5)	–0.52 (12.0)	–0.69 (10.75)
	Autumn	–0.96 (–1.5)	–0.98 (1.75)	–0.81 (8.5)	–0.81 (11.5)
	Winter	–0.96 (–1.5)	–0.97 (1.5)	–0.89 (6.5)	–0.89 (12.25)
E13	Spring	–0.94 (0.5)	–0.98 (2.5)	–0.70 (24.25)	–0.76 (19.25)
	Summer	–0.93 (0.25)	–0.98 (2.25)	–0.42 (15.25)	–0.59 (14.0)
	Autumn	–0.98 (–0.25)	–0.98 (3.0)	–0.84 (18.25)	–0.78 (22.25)
	Winter	–0.96 (–0.25)	–0.97 (2.75)	–0.82 (10.5)	–0.83 (16.5)
E17	Spring	–0.96 (0.0)	–0.98 (2.0)	–0.64 (27.25)	–0.73 (22.75)
	Summer	–0.96 (0.25)	–0.98 (2.0)	–0.34 (15.25)	–0.52 (14.25)
	Autumn	–0.99 (–0.75)	–0.98 (2.5)	–0.83 (19.5)	–0.78 (23.5)
	Winter	–0.96 (–0.5)	–0.98 (2.5)	–0.80 (11.5)	–0.81 (17.5)

It is obvious that the values of correlation coefficient for daily variation are all considerably higher than those for long-term variation. The possible reason may come from the fact that the length of continuous data for each season is restricted between 21 days to 30 days in this study and the long-term temperature effect can not be comprehensively assessed within such a limited interval. Furthermore, it is essentially true that the correlation coefficients obtained with the cable temperature are slightly better than those based on the air temperature, especially in the daily variation. As for comparing the effectiveness of this methodology in four different seasons, the values of correlation coefficient for the long-term variations in the summer are clearly inferior to the values corresponding to the other seasons. This phenomenon may be also resulted from the shortest period (21 days) of collected data for the summer case among all the four seasons.

6. Exclusion of temperature effect from variation of cable force

According to the results presented in the previous section, it is apparent that the daily and long-term components of temperature variation demonstrate either highly or moderately linear correlation with the corresponding components of cable force variation. Exploiting this feature, a recent work by the authors (Chen, Wu *et al*. 2016) made an effort to filter out the environmental temperature effect on the variation of cable force based on an effective temperature index. The technique of least square errors was applied to determine the two different transfer coefficients associated with the daily and long-term components of temperature variation for separating their possibly varied influences on the cable force variation. This approach is also adopted in this study, but only utilizing simple cable or air temperature measurements for the elimination of temperature effect.

Because the component of daily variation is usually with a dominant contribution and it is much more sensitive to the time shift than that of long-term variation, the optimal time shift $k\Delta t$ for the daily variation is taken for both components in the analysis to decide the transfer coefficients. At the time instant $t_i = i\Delta t$, assume that $z_i = z(t_i)$ represents the denoised cable force variation. Moreover, $x_{i-k} = x(t_i - k\Delta t)$ and $y_{i-k} = y(t_i - k\Delta t)$ denote the daily variation and the long-term variation of temperature with the same shift $k\Delta t$ along the time axis, respectively. To optimally exclude the effects of x_{i-k} and y_{i-k} from z_i in a linear manner, a transfer coefficient a_1 associated with the daily variation of temperature and another transfer coefficient a_2 associated with the long-term variation of temperature are to be determined such that the error between z_i and $a_1 x_{i-k} + a_2 y_{i-k}$ is minimized. With the data collected at n consecutive time instants t_0, t_1, …, t_{n-1}, an appropriate objective function for conducting the optimization procedures can be defined by the sum of the squares of the errors as

$$E = \sum_{i=k}^{n-1} \left[\left(z_i - \bar{z} \right) - a_1 \left(x_{i-k} - \bar{x} \right) - a_2 \left(y_{i-k} - \bar{y} \right) \right]^2 \quad (4)$$

where

$$\bar{z} = \frac{1}{n-k} \sum_{i=k}^{n-1} z_i \,, \quad \bar{y} = \frac{1}{n-k} \sum_{i=k}^{n-1} y_i \quad \text{and} \quad \bar{x} = \frac{1}{n-k} \sum_{i=k}^{n-1} x_i \quad (5)$$

Eq. (4) means that the linear regression analysis is performed by taking all the quantities with respect to the mean value of each variable. With this shift of reference point from the initial value to a more stable mean value, the possible problems induced by the inaccurate initial values due to measurement noises and the other minor factors to cause cable force variation can be alleviated. The detailed discussions for this optimization process can be referred to the previous work (Chen, Wu *et al*. 2016).

With the obtained transfer coefficients, the residual cable force variation after the elimination of temperature effect can be obtained by $\left(z_i - \bar{z} \right) - a_1 \left(x_{i-k} - \bar{x} \right) - a_2 \left(y_{i-k} - \bar{y} \right)$ or $z_i - a_1 x_{i-k} - a_2 y_{i-k} - \left(\bar{z} - a_1 \bar{x} - a_2 \bar{y} \right)$ for all the three stay cables in each season. Taking the data of Cable E13 measured in four different seasons for example, the values of residual cable force variation at different time instants are plotted in Figs. 14 to 17 with red crosses and their corresponding values before the elimination of temperature effect are also shown in grey dots. Figs. 14(a) and 14(b) evidently demonstrate that the range of cable force variation in the spring is significantly reduced roughly from 6% to 3% with the elimination of temperature effect in either the case adopting the air temperature or the case using the cable temperature. Such a reduction is principally due to the high correlation between the daily components and also assisted by the moderate correlation between the long-term components. In other words, the residual cable force variation majorly consists of the high-frequency noises and the remained long-term components not exclusively filtered out. More specifically, the adoption of cable temperature performs a little better for excluding the temperature effect. This tendency can be explained by the higher correlation coefficient either for the daily variation or the long-term variation associated with the cable temperature, as listed in Table 1. For further comparison, the other case employing the effective temperature index previously proposed by the authors (Chen, Wu *et al*. 2012, Chen, Wu *et al*. 2016) to combine the temperature contributions from the cable, pylon and girder is also presented in Fig. 14(c). It is observed that either the range of the residual cable force variation or its long-term fluctuation seems to be further suppressed in this case. Similar trends are also verified by the examination of Figs. 15 to 17 for the other three seasons. No clear difference, however, can be recognized between the performance with the cable temperature and that with the air temperature for the cases in the autumn and in the winter. Again, this phenomenon can be justified by the close values of correlation coefficient listed in Table 1 for these two seasons.

7. Conclusions

Very few works in the literature were able to practically asses the temperature effect on the cable force variation. An effective temperature index considering the detailed influences from different structural components was recently proposed by the authors to eliminate the environmental temperature effect from the variation of stay cable force. In the current work, simple cable or air temperature measurements are also found to be strongly correlated with the cable force variation. This feature unveils the possibility of employing the air or cable temperature to serve as a reliable temperature index for globally quantifying intricate temperature effects on low-pylon cable-stayed bridges. Using the data collected from Ai-Lan Bridge located in central Taiwan, this work further applies the ensemble empirical mode decomposition to process the time histories of cable force, air temperature and cable temperature. For reducing the computation intensity of EEMD, the utilization of paired white noises with opposite values at each instant is introduced in this study.

It is evidently observed that the cable force and both types of temperature can all be categorized as the daily variation, long-term variation and high-frequency noise in the order of decreasing weight. Moreover, the correlation analysis conducted for the decomposed variations of all these three quantities undoubtedly indicates that the daily and long-term variations with different time shifts have to be distinguished for accurately evaluating the temperature effect on the variation of cable force. Consistent results confirm the validity and stability of the developed method. The nearly perfect correlation between the daily variations of the cable force and the air temperature (or the cable temperature) is obtained for all the four seasons and all the three inspected stay cables. Even though the cases of long-term variation do not hold a correlation as strong as those of daily variation, elimination of temperature effect from the cable force variation can still be effectively conducted. The inferiority of long-term components may come from the fact that the length of the continuous time histories is not adequate to fully reflect the variation of the long-term effect.

In general, the residual cable force variations of different cases can be consistently reduced to a narrow range of 3% if either the air or cable temperature is utilized to perform the exclusion of temperature effect. Since the performance with the air temperature is found to be no worse than that with the cable temperature in several investigated cases, the air temperature which is usually handy at or near the bridge site may be considered a favorable choice in engineering practice. Comparison is also made to observe that the residual cable force variations based on the effective temperature index typically fall into a relatively narrower range. Therefore, the more convenient approach simply based on the air or cable temperature measurement requires lower monitoring costs, but is with a slight trade-off in sensitivity. The proposed method in this research offers a feasible and practical solution for eliminating the environmental effect on the cable force variation and the subsequent health monitoring of low-pylon cable-stayed bridges. It is hoped that a much longer period of continuous measurements without the interruption of technical difficulties can be attained in the future for different cable-stayed bridges to more convincingly investigate the long-term correlation and verify the broad applicability of this methodology. As for the other type of cable system such as the main cables or the vertical suspenders of a suspension bridge, it is not within the scope of this study and will need to be further explored.

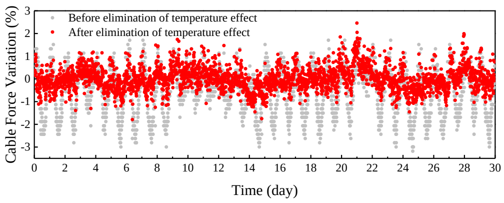

(a) Air temperature

Continued-

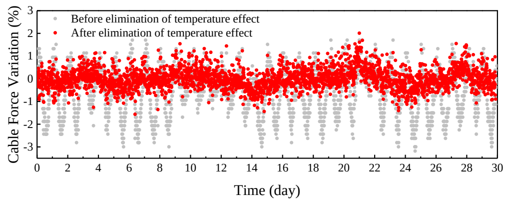

(b) Cable temperature

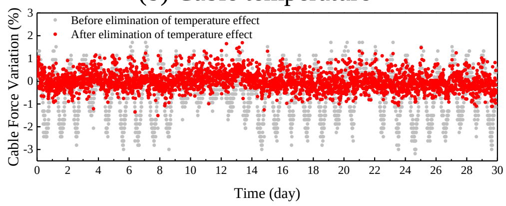

(c) Effective temperature

Fig. 14 Residual cable force variation of Cable E13 in the spring

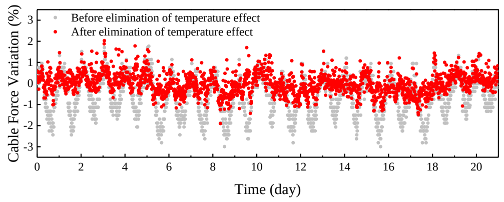

(a) Air temperature

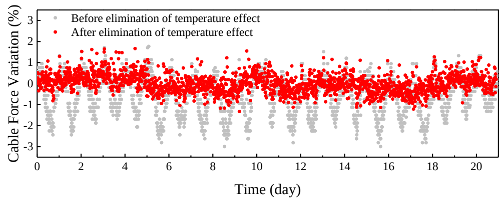

(b) Cable temperature

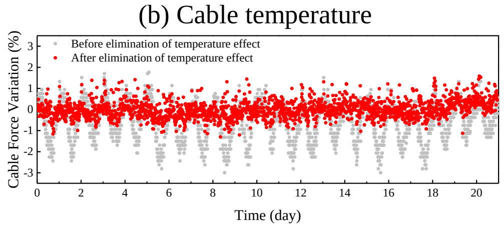

(c) Effective temperature

Fig. 15 Residual cable force variation of Cable E13 in the summer

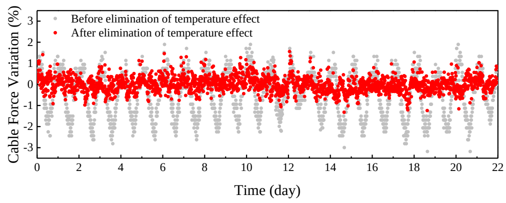

(a) Air temperature

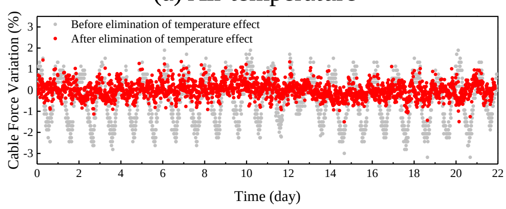

(b) Cable temperature

Continued-

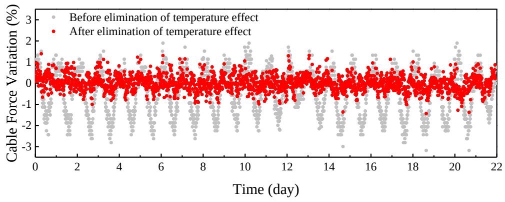

(c) Effective temperature

Fig. 16 Residual cable force variation of Cable E13 in the autumn

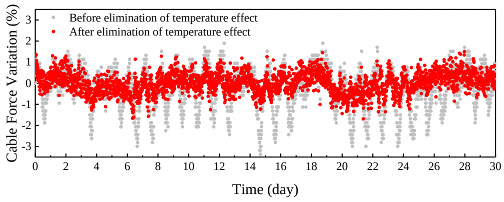

(a) Air temperature

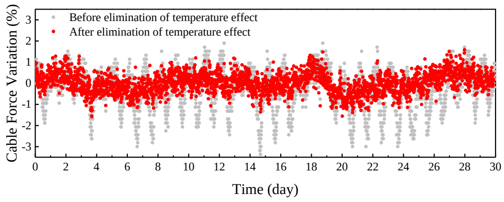

(b) Cable temperature

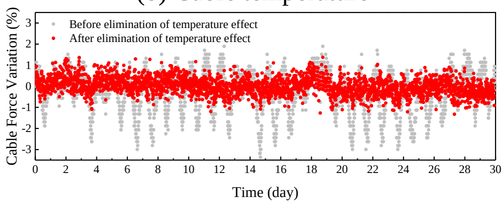

(c) Effective temperature

Fig. 17 Residual cable force variation of Cable E13 in the winter

Acknowledgments

The authors are grateful to Taiwan Area National Freeway Bureau, Ministry of Transportation and Communications of Republic of China, for its assistance in conducting the measurements of this study. The financial support from the Ministry of Science and Technology of Republic of China under Grant NSC 101-2221-E-224 -061 is also much appreciated.

References

Bagherzadeh, S.A. and Sabzehparvar M. (2015), "A local and online sifting process for the empirical mode decomposition and its application in aircraft damage detection", *Mech. Syst. Signal. Pr.*, **54**, 68-83.

Cao, Y.H., Yim, J.S., Zhao, Y. and Wang, M.L. (2011), "Temperature effects on cable stayed bridge using health monitoring system: a case study", *Struct. Health Monit.*, **10**(5), 523-537.

Chang, C.C. and Poon, C.W. (2010), "Nonlinear identification of lumped-mass buildings using empirical mode decomposition and incomplete measurement", *J. Eng. Mech. - ASCE*, **136**(3), 273-281.

Chen, C.C., Wu, W.H. and Liu, C.Y. (2012), "Effects of temperature variation on cable forces of an extradosed bridge", *Proceedings of the 6th European Workshop on Structural Health Monitoring*, Dresden, Germany, July**.**

Chen, C.C., Wu, W.H. and Shih, Y.D. (2010), "Effects of environmental variability on stay cable frequencies", *Proceedings of the 2nd International Symposium on Life-Cycle Civil Engineering*, Taipei, Taiwan, October.

Chen, C.C., Wu, W.H. and Tseng, H.Z. (2008), "Measurement of ambient vibration signal of shorter stay cables from stressing to service stages", *Proceedings of the 4th European Workshop on Structural Health Monitoring*, Krakow, Poland, July.

Chen, C.C., Wu, W.H., Liu, C.Y. and Lai, G. (2016), "Damage detection of a cable-stayed bridge based on the variation of stay cable forces eliminating environmental temperature effects", *Smart Struct. Syst.*, **17**(6), 859-880.

Chen, J. (2009), "Application of empirical mode decomposition in structural health monitoring: some experience", *Adv. Adapt. Data Anal.*, **1**(4), 601-621.

Cunha, A., Caetano, E., Magalhaces, F. and Moutinho, C. (2013), "Recent perspectives in dynamic testing and monitoring of bridges", *Struct. Control. Health. Monit.*, **20**(6), 853-877.

Degrauwe, D., De Roeck, G. and Lombaert, G. (2009), "Uncertainty quantification in the damage assessment of a cable-stayed bridge by means of fuzzy numbers", *Comput. Struct.*, **87**(17-18), 1077-1084.

Ding, Y.L., Wang, G.X., Zhou, G.D. and Li, A. (2013), "Life-cycle simulation method of temperature field of steel box girder for Runyang cable-stayed bridge based on field monitoring data", *China Civil Eng. J.*, **46**(5), 129 136.

Dohler, M., Hille, F., Mevel, L. and Rucker, W. (2014), "Structural health monitoring with statistical method during progressive damage test of S101 bridge", *Eng. Struct.*, **69**, 183-193.

Dong, Y.F., Li, Y.M. and Lai, M. (2010), "Structural damage detection using empirical-mode decomposition and vector autoregressive moving average model", *Soil Dyn. Earthq. Eng.*, **30**(3), 133-145.

He, X.H., Hua, X.G., Chen, Z.Q. and Huang, F.L. (2011), "EMD-based random decrement technique for modal parameter identification of an existing railway bridge", *Eng. Struct.*, **33**(4), 1348-1356.

Hu, J.S., Yang, S.X. and Ren, D.Q. (2008) "Study on the method of EMD-based vibration signal time-frequency analysis", *J. Vib. Shock*, **27**(8), 71-73.

Huang, N.E., Shen, Z., Long, S.R., Wu, M.C., Shih, H.H, Zheng, Q.A., Yen, N.C., Tung, C.C. and Liu, H.H. (1998), "The empirical mode decomposition and the hilbert spectrum for nonlinear and non-stationary time series analysis", *Proc. R. Soc. London Ser. A*, **454**, 903-995.

Lee, Z.K., Wu, T.H. and Loh, C.H. (2003), "System identification on the seismic behavior of an isolated bridge", *Earthq. Eng. Struct. D.*, **32**(12), 1797-1812.

Li, D.S., Ou, J.P., Lan, C.M. and Li, H. (2012) "Monitoring and failure analysis of corroded bridge cables under fatigue loading using acoustic emission sensors", *Sensors*, **12**(4), 3901-3915.

Li, H., Ou, J.P. (2016), "The state of the art in structural health monitoring of cable-stayed bridges", *J. Civil Struct. Health Monit.*, **6**(1), 43-67.

Li, H., Ou, J.P. and Zhou, Z. (2009), "Applications of optical fibre Bragg gratings sensing technology-based smart stay cables", *Opt. Lasers Eng.*, **47**(10), 1077-1084.

Li, H.J. (2009), "Temperature effect analysis for structural state estimation of PC cable-stayed bridge", *Archit. Env. Eng.*, **31**(5), 81-85.

Li, S.L., Li, H., Liu, Y., Lan, C.M., Zhou, W.S. and Ou, J.P. (2014), "SMC structural health monitoring benchmark problem

using monitored data from an actual cable-stayed bridge", *Struct. Control Health Monit.*, **21**(2), 156-172.
Lin, J.W. (2011) "A hybrid algorithm based on EEMD and EMD for multi-mode signal processing", *Struct. Eng. Mech.*, **39**(6), 813-831.
Min, Z.H., Sun, L.M. and Dan, D.H. (2009), "Effect analysis of environmental factors on structural modal parameters of a cable-stayed bridge", *J. Vib. Shock*, **28**(10), 99-105.
Min, Z.H., Sun, L.M. and Zhong, Z. (2011), "Effect analysis of environmental temperature on dynamic properties of cable-stayed bridge", *J. Tongji. U.*, **39**(4), 488-494.
Ni, Y.Q., Hua, X.G., Fan, K.Q. and Ko, J.M. (2005), "Correlating modal properties with temperature using long-term monitoring data and support vector machine technique", *Eng. Struct.*, **27**(12), 1762-1773.
Ni, Y.Q., Hua, X.G., Wong, K.Y. and Ko, J.M. (2007), "Assessment of bridge expansion joints using long-term displacement and temperature measurement", *J. Perform Constr. Facil. - ASCE*, **21**(2), 143-151.
Ni, Y.Q., Zhou, H.F. and Ko, J.M. (2009), "Generalization capability of neural network models for temperature-frequency correlation using monitoring data", *J. Struct. Eng. - ASCE*, **135**(10), 1290-1300.
Ni, Y.Q., Zhou, H.F., Chan, K.C. and Ko, J.M. (2008), "Modal flexibility analysis of cable-stayed Ting Kau bridge for damage identification", *Comput.-Aided Civ. Infrastruct. Eng.*, **23**(3), 223-236.
Pai, P.F. (2013), "Time-frequency analysis for parametric and non-parametric identification of nonlinear dynamical systems", *Mech. Syst. Signal. Pr.*, **36**, 332-353.
Rezaei, D. and Taheri, F. (2011), "Damage identification in beams using empirical mode decomposition", *Struct. Health Monit.*, **10**(3), 261-274.
Trker, T. and Bayraktar, A. (2014), "Structural safety assessment of bowstring type RC arch bridges using ambient vibration testing and finite element model calibration", *Measurement*, **58**, 33-45.
Whelan, M.J. and Janoyan, K.D. (2010) "In-service diagnostics of a highway bridge from a progressive damage case study", *J. Bridge Eng. - ASCE*, **15**(5), 597-607.
Wu, Z.H. and Huang, N.E. (2009), "Ensemble empirical mode decomposition: a noise-assisted data analysis method", *Adv. Adapt. Data Anal.*, **1**(1), 1-41.
Yang, Y.B. and Chang, K.C. (2009), "Extraction of bridge frequencies from the dynamic response of a passing vehicle enhanced by the EMD technique", *J. Sound Vib.*, **322**(4-5), 718-739.
Yu, D.J. and Ren, W.X. (2005), "EMD-based stochastic subspace identification of structures from operational vibration measurements", *Eng. Struct.*, **27**(12), 1741-1751.
Zhang, X., Du, X.L. and Brownjohnm, J. (2012), "Frequency modulated empirical mode decomposition method for the identification of instantaneous modal parameters of aeroelastic systems", *J. Wind Eng. Ind. Aerod.*, **101**, 43-52.
Zhou, H.F., Ni, Y.Q. and Ko, J.M. (2010), "Constructing input to neural networks for modeling temperature-caused modal variability: mean temperatures, effective temperatures, and principal components of temperatures", *Eng. Struct.*, **32**(6), 1747-1759.
Zhou, H.F., Ni, Y.Q. and Ko, J.M. (2012), "Eliminating temperature effect in vibration-based structural damage detection", *J. Eng. Mech. - ASCE*, **137**(12), 785-796.

CY